Rotational Dynamics of the Regulatory Light Chain in Scallop Muscle Detected by Time-Resolved Phosphorescence Anisotropy

Sampath Ramachandran and David D. Thomas*

Department of Biochemistry, University of Minnesota Medical School, Minneapolis, Minnesota 55455

Received February 8, 1999; Revised Manuscript Received May 4, 1999

ABSTRACT: We have used time-resolved phosphorescence anisotropy (TPA) to study the rotational dynamics of chicken gizzard regulatory light chain (RLC) bound to scallop adductor muscle myofibrils in key physiological states. Native RLC from scallop myofibrils was extracted and replaced completely with gizzard RLC labeled specifically at Cys 108 with erythrosin iodoacetamide (ErIA). The calcium sensitivity of the ATPase activity of the labeled myofibril preparation was quite similar to that of the native sample, indicating that the ErIA-labeled RLC is functionally bound to the myosin head. In rigor (in the absence of ATP, when all the myosin heads are rigidly bound to the thin filament), a slight decay was observed in the first few microseconds, followed by no change in the anisotropy. This indicates small-amplitude restricted motions of the RLC or the entire LC domain of myosin. Addition of calcium to rigor restricts these motions further. Relaxation with ATP (no Ca) causes a large decay in the anisotropy, indicating large-amplitude rotational motion with correlation times of 5−50 μs. Further addition of calcium, to induce contraction, resulted in a decrease in the rate and amplitude of anisotropy decay. In particular, there is clear evidence for a slow rotational motion with a correlation time of approximately 300 μs, which is not present either in rigor or relaxation. This indicates rotational motion that specifically correlates with force generation. The changes in the rotational dynamics of the light-chain domain in rigor, relaxation, and contraction support earlier work based on probes of the catalytic domain that muscle contraction is accompanied by a disorder-to-order transition of the myosin head. However, the motions of the LC domain are different from those of the catalytic domain, which indicates rotation of the two domains relative to each other.

ATP[1]-dependent sliding of myosin filaments over actin is the basis for force generation in muscle (*1*). On the basis of electron micrographic cross-sections of skeletal muscle (*2*−*4*) and structural, mechanical, and kinetic data (*5*−*7*), it has been proposed that force generation and muscle contraction are caused by ATP-driven rotational motions of cross-bridges formed by myosin heads binding to actin. Since the initial proposal of the rotating cross-bridge model, an array of biophysical techniques has been used to study the molecular basis of this process. Techniques such as electron microscopy (*8*−*10*), X-ray diffraction (*11*), and small-angle X-ray scattering (*12*) have suggested that the only distinct cross-bridge orientation is that in rigor, in the absence of ATP.

Site-directed probe techniques, involving primarily electron paramagnetic resonance (EPR) and optical spectroscopy, have provided orientational and motional sensitivity (*13*). Most of these studies have involved the attachment of probes to a reactive sulfhydryl group, SH1 (Cys 707 in rabbit), on the myosin head's catalytic domain. These studies indicate the cross-bridge cycle to be dynamic, with myosin heads undergoing sub-millisecond rotational motions even when attached to actin during the ATPase cycle (*14*−*16*). Contrary to earlier proposals (*3*, *4*), the orientation of the catalytic domain does not appear to be rigidly coupled to the ATPase cycle, and probes on SH1 do not show evidence for two distinct head orientations during the cycle (*13*, *17*−*20*). However, significant limitations remain in these studies: (a) SH1 labeling has been shown to partially inhibit actomyosin ATPase activity and fiber force (*21*, *22*) and (b) SH1 may not be representative of the whole cross-bridge (*18*, *23*). This latter conclusion is supported by the crystal structures of myosin S1 (*24*, *25*).

The high-resolution structure of the myosin head suggests the presence of two distinct domains, the catalytic or motor domain, containing the SH1, the ATP, and actin binding sites,

† Supported by grants from the Muscular Dystrophy Association, NIH (AR32961), NSF (DIR-9113444), and the Minnesota Supercomputer Institutes. S.R. was supported by a neuromuscular disease postdoctoral research fellowship from the Muscular Dystrophy Association.

* To whom correspondence should be addressed: Department of Biochemistry, Molecular Biology, and Biophysics,University of Minnesota Medical School, Minneapolis, MN 55455. E-mail: ddt@ddt.biochem.umn.edu. Phone: (612) 625-0957. Fax: (612) 624-0632.

[1] Abbreviations: AA, amino acid; ATP, adenosine triphosphate; CP, creatine phosphate; CPK, creatine phosphokinase; DTT, dithiothreitol; E5M, eosin-5-maleimide; EDTA, ethylenediamine *N*,*N*,*N*′,*N*′-tetraacetic acid; EGTA, ethyleneglycol-bis-(β-aminoethyl ether)*N*,*N*,*N*′,*N*′-tetraacetic acid; EPR, electron spin resonance; ELC, essential light chain; ErIA, erythrosin iodoacetamide; FDNA-SL, 3-(5-fluoro-2,4-dinitroanilino)-2,2,4,4-tetramethyl-1-pyrrolidinyloxy spin label; kDa, kilodaltons; LC, light chain; Mops, 3-(*N*-morpholino)propanesulfonic acid; MHC, myosin heavy chain; MSL, *N*-(1-oxy-2,2,6,6-tetramethyl-4-piperidinyl)maleimide; PAGE, polyacrylamide gel electrophoresis; PMMA, poly(methyl methacrylate); RLC, regulatory light chain; SH1, Cys707 in the rabbit (or chicken) skeletal S1 sequence; SDS, sodium dodecyl sulfate; SEM, standard error of mean; ST-EPR, saturation transfer EPR; TPA, time-resolved phosphorescence anisotropy.

10.1021/bi9902945 CCC: $18.00
Published on Web 06/19/1999

and the light-chain or regulatory domain, containing the essential and regulatory light chains (*24*, *25*). Models based on this structure have proposed that the key event in muscle contraction is the rotation of the LC domain relative to the catalytic domain (*25*−*27*). In fact, considerable cross-bridge distortion has been seen both by electron microscopy (*28*−*30*) and X-ray diffraction (*25*, *30*), suggesting that substantial flexibility is present in the myosin head and that this might be coupled to force generation (*31*, *32*). To test this "bending head" hypothesis (*18*, *23*), it is necessary to probe directly the orientation and rotational motions of both the catalytic and light-chain domains in muscle.

The obvious targets for introducing spectroscopic probes in the LC domain of the myosin head are on the RLC subunits. In principle, probes could be attached directly and selectively to the heavy chain part of the LC domain, but this has proven to be a formidable challenge, due to the lack of a unique high-affinity reactive group. On the other hand, the RLC binds specifically and noncovalently the heavy chain and can be removed and exchanged by altering the ionic conditions. There are two distinct advantages in studying scallop muscle: (a) the native RLC can be easily removed and replaced with any other RLC, and (b) the functional binding of exogeneous RLC can be readily monitored by measuring the calcium sensitivity of ATPase activity (*33*, *34*). The gizzard RLC contains a single cysteine (Cys 108) for site-specific attachment of the probe, and it restores calcium sensitivity to scallop muscle.

Two recent papers have reported EPR of spin labels bound to RLC in contracting scallop muscle. Using the high orientational resolution of conventional EPR, Baker et al. (*32*) obtained the first direct evidence for two distinct orientations of the LC domain in muscle and showed that a change in the distribution between these two orientations correlates with force generation. Using saturation-transfer EPR to obtain sensitivity to microsecond rotational motions, Roopnarine et al. (*35*) showed that the orientational changes occurring upon contraction are accompanied by a reduction in microsecond rotational motion. However, neither of these EPR techniques had the time resolution needed to detect and resolve the distinct rotational motions that might be occurring in different phases of the force generation process.

In the present study, we report time-resolved phosphorescence anisotropy (TPA) experiments on scallop adductor muscle myofibrils containing erythrosin-labeled chicken gizzard RLC, to study the rotational motion of the LC domain of myosin in different physiological states. Phosphorescence was used in order to obtain information on the crucial microsecond time range, as demonstrated in previous TPA studies of SH1-bound probes in rabbit myofibrils (*36*) and fibers (*37*). The present TPA study provides the first time-resolved data on LC domain rotational motion and reveals changes in cross-bridge dynamics upon contraction that were not previously detected.

MATERIALS AND METHODS

Reagents and Solutions. Erythrosin iodoacetamide (ErIA) was obtained from Molecular Probes (Eugene, OR) and stored at a concentration of 200 mM in dimethylformamide (DMF) in liquid nitrogen. Catalase, glucose oxidase, glucose, ATP, creatine phosphate (CP), and creatine phosphokinase (CPK) were from Sigma (St. Louis, MO). All other chemicals were of the highest available purity. Live scallops were obtained from Marine Biological Laboratories, Woodshole, MA. The scallops were kept alive in a tank for up to six months. The following solutions were used in our experiments: labeling solution (LS) (100 mM NaCl, 2 mM EDTA, 20 mM MOPS, pH 7), magnesium wash (MW) (40 mM NaCl, 1.5 mM EGTA, 3 mM NaN_3, 2 mM $MgCl_2$, 10 mM Mops, pH 7), sodium azide wash (AW) (40 mM NaCl, 1.5 mM EGTA, 3 mM NaN_3, 10 mM Mops, pH 7), rigor solution without backup (R) (84 mM KPr, 2 mM $MgCl_2$, 1.5 mM EGTA, 20 mM Mops, pH 7), rigor solution with backup (RB) (R plus 0.1 mg/mL CPK + 20 mM CP), relaxation solution (RE) (RB plus 5 mM ATP), contraction solution (RE plus 2 mM $CaCl_2$).

Preparation and Labeling of Gizzard RLC. Myosin was partially purified from frozen gizzards by the method of Persechini and Hartshorne (*38*). A mixture of essential and regulatory light chains was prepared from the myosin by the method of Wagner (*39*). Ethanol was then added to a final concentration of 82% to precipitate the RLC which was then resuspended and dialyzed into 0.1 M NaCl, 50 mM Tris, pH 7.9, 0.1 mM each of EGTA and EDTA, 0.5 μg/mL each of pepstatin A and leupeptin, and 1 mM DTT. After dialysis, sucrose was added to 25% (w/v) and the RLC was stored in liquid nitrogen for up to nine months. For labeling with ErIA, the RLC was thawed and DTT was added to 5 mM. After 30 min, the RLC was dialyzed into 2 L of LS for 5 h. Labeling was initiated by adding 1.5 times molar excess of ErIA in labeling buffer to the RLC. After 20 h on ice, free label was removed on a Sephadex G-25 column primed with MW. The labeled RLC was then concentrated in Centricon centrifugal concentrators. The amount of label attached to the protein was calculated by measuring the absorbance at 530 nm using a molar extinction coefficient of 72 600/M/cm. Extinction coefficient of the dye attached to the protein was measured by adding a known concentration of the dye to a 10-fold excess of the RLC and then measuring the absorbance at 530 nm. The protein concentration was determined using the Bradford assay (*40*). The dye-to-protein ratio was 0.80 ± 0.08 ($n = 7$, SEM).

Preparation of Scallop Myofibrils, Extraction of Native RLC, and Reconstitution with Gizzard RLC. Striated adductor muscle was prepared from *Placopecten magellanicus* (bay scallop) after removing all the catch muscle. The muscle was then stored in 50% ethylene glycol (v/v) for up to 1 year. Myofibrils were made by grinding small pieces of muscle in magnesium wash with a tissuemizer. The membrane debris was removed by washing with MW. Then the myofibrils were suspended in AW. The protein concentration was adjusted to 3 mg/mL, and EDTA was added to 15 mM. After a 10 min incubation, the myofibrils were immediately washed with AW at room temperature to remove the extracted native RLC, then washed with MW (*33*). Reconstitution with the labeled gizzard RLC was started by adding five times molar excess of erythrosin-labeled gizzard RLC over myosin. After 8−12 h, the unbound RLC was removed by washing with MW. The myofibrils were not cross-linked and, hence, underwent some shortening during contraction.

Gel Electrophoresis. Myofibril samples were analyzed on a 12.5% (w/v) polyacrylamide gel containing 8 M urea at pH 8.6. Myofibrils were incubated in a equal volume of

sample buffer containing 8 M urea for 2 h at room temperature. Then 20 μg aliquots were loaded into the gel. The gels were stained with Coomassie Brilliant Blue R-250 and scanned in a phosphorimager and the density of the protein bands were quantitated.

ATPase Activity. The ATPase activities of the myofibrils were measured by monitoring the inorganic phosphate release (*41*). Relaxation buffer: 20 mM KCl, 1 mM $MgCl_2$, 1.5 mM EGTA, and 25 mM Mops, pH 7.5. Activation buffer: 20 mM KCl, 1 mM $MgCl_2$, 1.5 mM EGTA, 1 mM $CaCl_2$, and 25 mM Mops.

Optical Spectroscopy. For phosphorescence experiments, the labeled myofibril samples were diluted to 0.3 mg/mL with RB in a cuvette. Oxygen was removed from the sample by the addition of 100 μg/mL glucose oxidase, 15 μg/mL catalase, and 5 mg/mL β-D-glucose (*36*). Deoxygenation was allowed to proceed for a few minutes before data collection. For relaxation experiments, ATP was added to myofibrils in RB, and for contraction, $CaCl_2$ was added to relaxed myofibrils. The samples were incubated for a few minutes after each addition, and the TPA was then measured. No significant settling of the myofibrils was observed during data collection as measured by light scattering at 660 nm. The anisotropy is defined as

$$r(t) = (I_{vv} - GI_{vh})/(I_{vv} + 2GI_{vh}) \quad (1)$$

where I_{vv} and I_{vh} are the vertical and horizontal components of the emission after excitation with a vertically polarized pulse. TPA decays were recorded using an instrument described previously (*36*), by signal averaging the time-dependent phosphorescence decays with a single detector and a polarizer that alternates between vertical [$I_{vv}(t)$] and horizontal [$I_{vh}(t)$] orientation every 1000 flashes. G is an instrumental correction factor, determined by measuring the anisotropy of a solution of ErIA-labeled BSA in 90% glycerol (v/v) under experimental conditions and adjusting G to give an anisotropy value of zero, the theoretical value for a freely tumbling chromophore.

Analysis of Anisotropy Data. TPA decays were analyzed by fitting them to theoretical expression, using the nonlinear least-squares algorithm of Marquardt (*42*). The quality of the fits were gauged by comparing the χ^2 values and by evaluating the residuals. The total intensity, $I(t)$, was fit to the expression

$$I(t) = \sum_{i=1}^{n} a_i \exp(-t/\tau_i) \quad (2)$$

where τ_i is the excited-state lifetime for component i. The anisotropy decay was fit to a sum of exponentials plus a constant (*36*)

$$r(t) = \sum_{i=1}^{n} r_i \exp(-t/\phi_i) + r_\infty \quad (3)$$

where r_0 is the initial anisotropy at time zero, ϕ_i is the rotational correlation time for component i, and r_∞ is the final anisotropy. The number of exponentials (n in eq 2 and 3) was increased until no further improvement was observed in the fit, as evaluated by the χ^2 value (minimized in least-squares fit) and the residual plot (data minus fit). For total intensity (eq 2), we found that the fit was improved by increasing n from 3 to 4. For anisotropy (eq 3), $n = 2$ was usually both necessary and sufficient for an optimal fit.

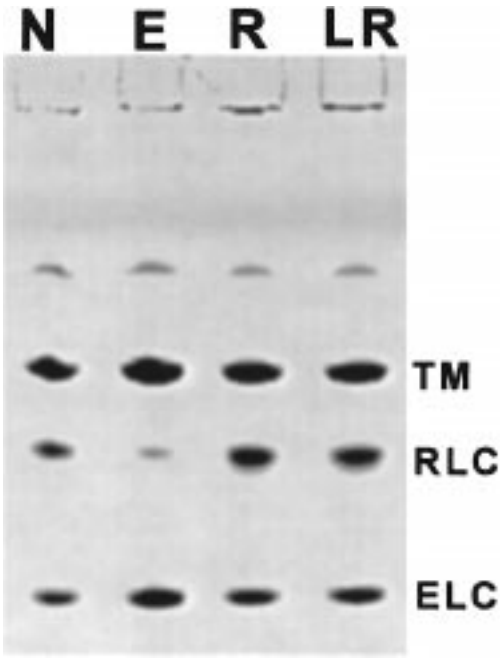

FIGURE 1: Urea polyacrylamide gel electrophoresis of scallop myofibril samples. Scallop myofibrils samples were analyzed on a 12.5% (w/v) gel. N, native myofibrils; E, extracted; R, reconstituted with native gizzard RLC; LR, reconstituted with ErIA labeled gizzard RLC. TM, tropomyosin; ELC, essential light chain; RLC, regulatory light chain.

We modeled the dynamic disorder of the emission transition moment of the probe in the nanosecond and the microsecond time ranges as a wobble in a cone with a semiangle of θ_c (*43*), which is calculated either from the microsecond order parameter, $S(\mu s)$, or the nanosecond-order parameter, S(ns):

$$S(\mu s) = \sqrt{r_\infty/r_0},\ S(ns) = \sqrt{r_0/r_{max}} \quad (4)$$

$$\theta_c = \cos^{-1}(-0.5 + 0.5\sqrt{1 + 8S}) \quad (5)$$

where r_0 and r_∞ are the initial and final anisotropies, respectively, as defined in eq **3**, and r_{max} is the anisotropy of the completely immobilized dye, measured by performing TPA on ErIA immobilized in a PMMA block. Thus, the difference between r_0 and r_{max} is due to the sub-microsecond rotational motion that is not detected by TPA. The submicrosecond decay is also quantitated as κ, which is defined as r_0/r_{max}. We measured r_{max} for ErIA as 0.20 ± 0.01. Thus, the amplitudes of microsecond motion, $\theta_c(\mu s)$, and submicrosecond motion, θ_c(ns), can be calculated from eqs 4 and 5.

RESULTS

Gel Electrophoresis. Urea−PAGE was used to determine the extent of RLC extraction and reconstitution in scallop myofibrils (Figure 1, Table 1). Since the ELC is not removed under the conditions of RLC extraction, it was used as a standard to normalize the RLC content. In native myofibrils, approximately equimolar amounts of the two light chains are present, and extraction removes greater than 90% of the

Table 1: ATPase Activity of Scallop Myofibrils[a]

sample	RLC/ELC	activity (IU) −Ca	activity (IU) +Ca	calcium sensitivity
native myofibrils	0.96 ± 0.04	0.03 ± 0.007	1.03 ± 0.03	0.97
extracted myofibrils	0.07 ± 0.01	0.52 ± 0.03	0.45 ± 0.02	−0.16
with gizzard RLC	0.94 ± 0.07	0.07 ± 0.02	0.97 ± 0.06	0.95
with ErIA-labeled RLC	0.97 ± 0.05	0.09 ± 0.02	0.96 ± 0.05	0.92

[a] ATPase activities [μmol of $P_i \cdot min^{-1} \cdot (mg\ of\ protein)^{-1}$], were measured at 25 °C in the media described in Materials and Methods. Each value is the mean from five different preparations, and the SEM is given. Calcium sensitivity = $[1 - (V(-Ca)/V(+Ca)] \times 100$. The intensities of the RLC bands were adjusted for their respective molecular masses: scallop RLC, 17 kDa; gizzard RLC, 20 kDa; and normalized to the ELC band intensity.

native RLC (Table 1). Upon readdition of either unlabeled or ErIA-labeled gizzard RLC, the content was restored to the native level, i.e., one RLC per myosin head (Table 1).

ATPase Activity. The native myofibril preparation shows a 34-fold increase of ATPase activity in the presence of calcium (Table 1). The extraction of more than 90% of RLC results in a high ATPase activity in the absence of calcium and a 13% decrease in its presence, indicating the loss of calcium regulation. Reconstitution with either gizzard RLC or ErIA-labeled gizzard RLC restores the regulation to near native values both in the absence and presence of calcium. This clearly indicates that greater than 90% of the heads in these myofibrils have labeled RLC that is bound functionally and stereospecifically to the myosin. Since the Urea−PAGE indicates stoichiometric binding of labeled RLC to myosin heads, we also conclude that greater than 90% of the labeled RLC is bound functionally to myosin.

Phosphorescence Intensity Decay. The unpolarized phosphorescence emission intensity decay, $I(t)$, of labeled scallop myofibrils does not depend significantly on the presence of ATP or Ca (Figure 2). These curves do not decay to zero in 500 μs, due to the long lifetime of phosphorescence emission. The results of three-exponential fits of these curves are shown in Table 2. ATP and/or calcium cause only small changes in amplitudes (α_i) and lifetimes (τ_i), which are not enough to account for the large differences in anisotropy decays reported below (*37*, *44*). The multiexponential nature of the decay suggests environmental heterogeneity, but not necessarily site heterogeneity, since multiexponential decays have been observed in most previous studies of protein-bound phosphorescent dyes, including purified myosin labeled at specifically at SH1 either with E5M or ErIA (*36*).

Phosphorescence Anisotropy: *Effect of ATP and Ca*. The anisotropy decays during rigor, relaxation, and contraction are shown in Figure 3. In the absence of ATP (rigor), a small decay is seen from 0 to 50 μs. This indicates restricted fast motion of the probe at the RLC. After the initial decay, there is very little change in anisotropy, with a slight rise in the anisotropy at longer times. A similar rise in anisotropy has also been seen in TPA of rabbit psoas myofibrils (*36*) and fibers (*37*). This is probably due to lifetime heterogeneity of the emission. If the short lifetime component has a smaller constant value for the anisotropy than a longer lifetime component, then the changing weighted average of the two components will give a rising anisotropy. In any case, it is obvious that the probe undergoes very limited motion in rigor. A single exponential (eq 3, $n = 1$) was insufficient to fit the decay, but two exponentials produced an adequate fit (Table 3). The small amplitude of TPA decay implies a small amplitude of rotational motion.

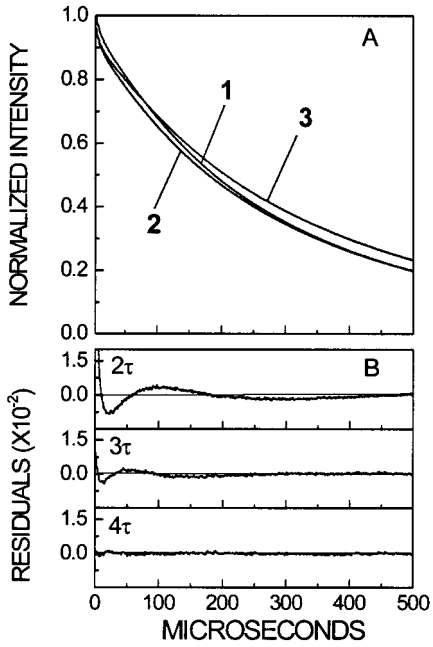

FIGURE 2: (A) Phosphorescence intensity decays of scallop myofibrils samples containing ErIA-labeled gizzard RLC during rigor, relaxation and contraction, at 4 °C; **1**, rigor; **2**, relaxation; **3**, contraction. The data is that from a typical sample. The decays were fit to a sum of exponential (see Materials and Methods, eq 2). (B) For contraction, a four exponential fit was judged to be adequate from the residual plots. Both rigor and relaxation intensity decays were fit to four exponentials (residual plots not shown). The results of the fits are shown in Table 2.

Table 2: Phosphorescence Emission Decay Parameters for Scallop Myofibrils[a]

state	α_1	τ_1 (μs)	α_2	τ_2 (μs)	α_3	τ_3 (μs)	α_4	τ_4
rig	0.102	5.8	0.101	33	0.241	150	0.558	390
	(0.002)	(0.4)	(0.004)	(5)	(0.015)	(10)	(0.016)	(10)
rel	0.099	6	0.100	35	0.351	170	0.450	420
	(0.002)	(0.7)	(0.007)	(4)	(0.041)	(20)	(0.047)	(20)
con	0.099	5.5	0.089	32	0.169	150	0.643	420
	(0.002)	(0.1)	(0.001)	(1)	(0.006)	(10)	(0.008)	(10)

[a] Nonlinear least-squares fit of the phosphorescence intensity decay $I(t)$ to a sum of exponential decay terms with amplitudes α_i and excited-state lifetimes τ_i (eq 1). The values are averages of four experiments, with SEM in parentheses. A representative data set is shown in Figure 1. The table shows only the results for a three-exponential fit ($n = 4$ in eq 1), which was judged to be optimal on the basis of residual plots (not shown)

Relaxation, induced by the addition of 5 mM MgATP, causes a fast initial decay in the first 50 μs, followed by a slower decay until about 200 μs. The decay causes a large drop in the anisotropy, indicating large-amplitude rotational motions of the probe. As in rigor, a two-exponential fit was adequate as judged from the residual plots (not shown). As seen in Table 3, amplitudes r_1 and r_2, associated with the short (5 μs) and long (46 μs) correlation times, respectively, are very similar. The initial anisotropy (r_0) is lower than that of rigor, indicating substantial submicrosecond motion during

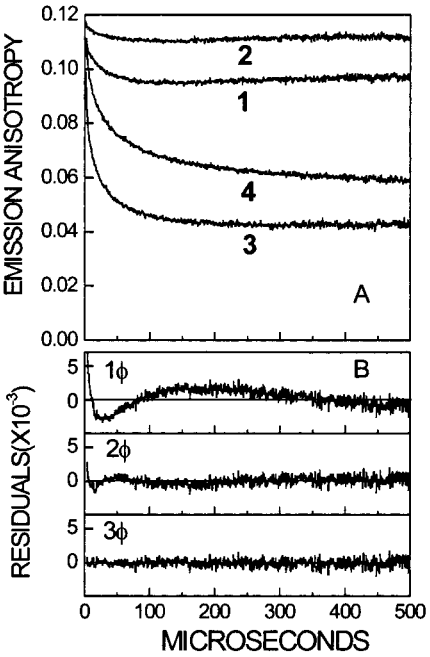

FIGURE 3: (A) Phosphorescence anisotropy decay of scallop myofibril samples containing ErIA-labeled gizzard RLC at 4 °C in **1**, Rigor; **2**, rigor plus 100 μM free calcium; **3**, relaxation; and **4**, contraction. Relaxation was initiated by adding 5 mM MgATP to rigor and contraction was started by adding 2 mM calcium chloride to relaxed myofibrils. A backup system of creatine phosphate and creatine kinase ensured that the ATP was always saturating during data acquisition. The data were fit to a sum of exponentials (see Materials and Methods, eq 3). (B) For the contraction decay, three exponentials were needed to fit the data as judged from the residuals. Rigor and relaxation were adequately fit to two exponentials (residuals not shown).

relaxation. The nonzero value of the final anisotropy (r_∞) shows that the rotational motion of the head is restricted in amplitude. During relaxation, the sub-microsecond motion is much greater than that seen in either rigor or contraction, as shown by a lower κ value (Table 3).

In contraction, the TPA decay is intermediate to those of rigor and relaxation (Figure 3A, Table 3), but three exponentials were required for an adequate fit, as shown in Figure 3B. The two shorter correlation times, ϕ_1 and ϕ_2, are almost identical to that in relaxation. The amplitudes, r_1 and r_2, associated with these correlation times are also similar. However the final anisotropy, r_∞, is higher than in relaxation, indicating that the overall rotational motion of the probe is more restricted. Another difference between the relaxation and contraction decay curves is a slow decay seen only in contraction. Whereas two exponentials were sufficient to fit rigor and relaxation, three were required to fit contraction (Figure 3B). The third unique decay component has a correlation time of about 300μs, which is about five times longer than that observed for rigor and relaxation.

Effect of Calcium in Rigor. The main effect of Ca is a slight decrease in the amplitude of the initial decay (Figure 3, Table 3), indicating greater restriction of the probe motion. However, no slow decay component like that in contraction was observed.

DISCUSSION

Specific and Functional Labeling of RLC. Contraction of scallop muscle is regulated by the binding of calcium to a high-affinity calcium-binding site in the essential light chain (*45*, *46*). Specific interactions of the ELC with the RLC and the myosin heavy chain are required for maintaining the structure of the calcium-binding site (*47*). Therefore, removing the RLC destroys calcium regulation (*33*), and rebinding of the RLC restores calcium binding and regulation. This functional reconstitution can be achieved with RLC either from other molluscan muscles or from a smooth muscle source such as chicken gizzard (*33*, *34*).

The urea−PAGE (Figure 1) and its densitometric analysis (Table 1) show that the ErIA-labeled gizzard RLC is stoichiometrically bound to the myofibrils, as observed in previous reconstitution studies on scallop myofibrils with unlabeled gizzard RLC (*34*). The ATPase rates in the absence and presence of calcium show that the ErIA-labeled gizzard RLC restores calcium sensitivity to scallop myofibrils, as observed previously with unlabeled gizzard RLC (*34*). Therefore, the labeling of the gizzard RLC has not affected the regulation of myosin ATPase by calcium in the myofibril samples. We conclude that *our spectroscopic data comes from myosin heads that are completely and specifically labeled with RLC that is functionally incorporated.* Although many studies have been carried out with probes bound to RLC in muscle, only those few studies carried out with scallop muscle (*32*−*35*) have achieved this level of complete, specific, and functional labeling, ensuring the reliable correlation of structure, dynamics, and function.

Interpretation of TPA Data in rigor. The TPA of ErIA-labeled gizzard RLC in scallop myofibrils exhibits a small but rapid decay, followed by no further change in the anisotropy. The small amplitude of the decay (Table 3) indicates small-amplitude rotational motion of the probe on the microsecond time scale: $\theta_c(\mu s)$, calculated from r_0 and r_∞ (eq 4), is about 20° (*43*). This amplitude of probe motion in rigor is greater than that of a phosphorescent probe at SH1 in rabbit skeletal muscle myofibrils (*36*) and fibers (*37*). This indicates that the LC domain of myosin has significant flexibility even when the myosin head is strongly bound to actin. The slight rotational motion in rigor is in agreement with saturation transfer EPR (ST-EPR) studies of scallop adductor muscle fibers containing spin-labeled clam (*Mercenaria*) regulatory light chain (*35*). The large residual anisotropy (r_∞) in rigor (Table 3) indicates that, despite some restricted rapid motion, the probe is static over most of the microsecond time range, in agreement with both ST-EPR (*49*) and TPA studies (*36*, *37*) with probes attached to SH1 in rabbit muscle, and with EPR studies of spin-labeled RLC in scallop muscle (*35*). Table 3 shows that there is also substantial probe rotational motion in the sub-microsecond time scale [θ_c(ns) = 33°] in rigor, probably due to fast probe wobble or to local motion of the amino acid side chain.

Binding of calcium to myosin heads in rigor causes a decrease in the amplitude of anisotropy decay (Figure 3), indicating restriction of probe rotation. From modeling studies of the crystal structure of scallop regulatory domain, Cohen and co-workers have predicted an increase in binding affinity of RLC to MHC upon binding of Ca during muscle contraction (*47*). When Cys108 of gizzard RLC is modeled into the structure of scallop regulatory domain, it is very close to Asp 22 of the ELC, which is directly involved in Ca binding at the high-affinity Ca-binding site. Thus, it is possible that binding of Ca causes a local effect at Cys108

Table 3: Phosphorescence Anisotropy Fit Parameters of Scallop Myofibrils in Different Physiological States[a]

state	r_1	ϕ_1 (μs)	r_2	ϕ_2 (μs)	r_3	ϕ_3 (μs)	r_∞	r_0	κ^c	θ_c (ns) (deg)[d]	θ_c (μs) (deg)[d]
rig[b]	0.007	3	0.012	28			0.096	0.114	0.57	34.5	19.2
	(0.001)	(1)	(0.001)	(2)			(0.002)	(0.003)	(0.2)	(1.5)	(0.7)
rel	0.033	5	0.033	46			0.042	0.101	0.51	37.5	42.1
	(0.001)	(0.3)	(0.001)	(2)			(0.001)	(0.001)	(0.4)	(1.2)	(0.8)
con	0.023	5	0.024	42	0.015	297	0.054	0.117	0.59	33.5	39.4
	(0.001)	(1)	(0.001)	(7)	(0.002)	(72)	(0.002)	(0.002)	(0.2)	(1.2)	(0.7)
rig + Ca	0.003	21					0.107	0.116	0.58	33.8	12.8
	(0.001)	(1)					(0.001)	(0.001)	(0.1)	(1.3)	(0.6)

[a] Nonlinear least-squares fit of the anisotropy decay $r(t)$ to a sum of exponential decay terms with amplitudes r_i and rotational correlation times ϕ_i. The values are averages from four experiments, with SEM in parentheses. Representative data sets are shown in Figure 3. Only results of the optimal fits are shown. They were judged to be optimal on the basis of the residual plots (Figure 3B). [b] rig, rigor; rig + Ca, rigor + calcium; rel, relaxation (−Ca); con, contraction (+Ca). [c] Calculated as described in the Materials and Methods. [d] Calculated assuming a wobble in a cone model (see Materials and Methods), where θ_c (ns) and θ_c (μs) are the semiangles of the cone calculated from the order parameters S_n and S_μ, respectively.

that restricts probe motion. A restriction of the motion of the whole LC domain upon Ca binding could have a similar effect. The effect of calcium on myosin heads in rigor is in contrast to SH1 probes in the catalytic domain, where no effect of calcium was seen. Thus, calcium binding inhibits rotational motion of the RLC or the LC domain relative to the catalytic domain.

Interpretation of TPA Data in Relaxation. The large anisotropy decay upon addition of ATP (Figure 3) shows that the LC domain undergoes large-amplitude rotational motions when the myosin heads are detached from or weakly attached to actin. Analysis of the TPA data using a wobble-in-cone model (*43*) yields a semiangle of $\theta_c(\mu s) = 43°$, more than twice the amplitude observed in rigor (Table 3). This result is consistent with large-amplitude microsecond motions detected in TPA and ST-EPR studies of myofibrils and fibers with probes attached to the SH1 site (Cys707 in rabbit) in the catalytic domain of myosin in myofibrils (*36*) and fibers (*15*, *20*, *37*, *49*). *Thus, the entire myosin head undergoes large-amplitude microsecond motions when weakly attached to actin or when completely detached from actin.* Relaxation also increases slightly the amplitude of nanosecond motion, compared to rigor and contraction, as evidenced by an increase in θ_c(ns) (Table 3). This is consistent with fluorescence polarization studies with probes on the RLC (*50*).

Interpretation of TPA Data in Contraction. The results in contraction are the most interesting aspect of this study. Upon addition of calcium to relaxed myofibrils, the most obvious changes are an increase in the final anisotropy (r_∞) compared to relaxation and a slow decay component with a long correlation time (about 300 μs) that is not found in rigor or relaxation (Figure 3, Table 3). The increase in the final anisotropy indicates that the stronger binding of myosin to actin decreases the angular amplitude of rotational motion (*36*, *37*). The decrease in the rate and amplitude of motion could be associated with the conformational changes within the RLC that are responsible for the myosin-based activation of scallop muscle (*51*). However, since the effect of Ca in rigor is much less than that observed upon activation (Figure 3), with no evidence for the 300 μs motion observed in contraction, *the new slow motion appears to be correlated specifically with force generation*; i.e., with the transition of myosin heads from weak to strong actin binding. It is not likely that the slow decay is associated with irreversible structural changes that take place in the myofibrils upon contraction, since the TPA decay of contracted myofibrils after ATP depletion reverts back to that seen in rigor (data not shown), indicating that the cross-bridges in thick filaments remain in full overlap with thin filaments, and major structural changes have not taken place in the myofibrillar array. In fact, most of the shortening probably takes place before data acquisition, so the cross-bridges within these contracting myofibrils are probably comparable to those in isometrically contracting fibers.

Due to the slowly decaying component, the TPA decay in contraction cannot be expressed as a linear combination of rigor and relaxation. This is in contrast with orientation studies with EPR probes at SH1 (*20*), fluorescent probes at the RLC (*52*), and EPR probes at the RLC (*32*), but it is in agreement with TPA studies with probes at SH1 in rabbit skeletal muscle myofibrils (*36*) and fibers (*37*). *Thus, TPA detects rotational motions that are unique to contraction both at the SH1 site in the catalytic domain and at the RLC in the LC domain.* Why are these unique properties of contracting myosin heads detected only by TPA? TPA is the only technique that has been applied to this problem that is capable of microsecond time resolution, measuring directly both the rates (inverse of correlation times) and amplitudes of rotational motion. This provides us with an important message—the essential physical properties of myosin heads that are responsible for force generation cannot be understood on the basis of static structural states. *Dynamics is crucial*: both the rates and amplitudes of rotational motions are needed to define the functionally crucial physical properties of myosin.

What fraction of the heads change their rotational dynamics upon activation? The time-resolution of TPA allows us to estimate this. The transition from relaxation to contraction corresponds primarily to the appearance of the slow (300 μs) component (amplitude r_3) and a decrease in the amplitudes of the two faster decay components (amplitudes r_1 and r_2 in Table 3). The simplest interpretation is to assign r_1 and r_2 to detached or weak-binding heads and r_3 to strong-binding heads that are actively attached to actin. The fraction of heads in this strong-binding state is then estimated to be $r_3/(r_1 + r_2 + r_3) = 24\%$.

Relationship to Other Spectroscopic Work on RLC. Spectroscopic studies with probes attached to the RLC have been done to understand the orientational and motional changes due to muscle contraction. Studies with FDNA-SL attached to RLC in rabbit skeletal muscle fibers indicate that the probes are oriented but undergo restricted rotation in rigor

(*53*). In relaxation, the probes are much more disordered than in rigor. These results are in agreement with our TPA data. However, in some cases, no change from relaxation was seen in contracting fibers (*54*, *55*). Fluorescence polarization studies in rabbit fibers indicate that while the probe is partially oriented in rigor, it has nearly random orientation in relaxation, and orientation in contraction is intermediate (*56*). However, due to the nanosecond lifetime of the fluorescent dye, no information was obtained about microsecond rotational motions. Large changes in the orientation of a fluorescent RLC probe in rabbit muscle fibers were detected upon relaxation, but little further change was seen in the active fibers (*50*, *57*). Our work has complemented these studies by resolving the motions of the RLC and the LC domain in the microsecond time scale. An ST-EPR study of the microsecond dynamics of the RLC in scallop muscle fibers, while consistent with the present TPA results, lacks both time and amplitude resolution of the dynamic motion (*35*). Since TPA offers both time and amplitude resolution of microsecond rotational motion, we have detected the presence of unique rotational motions in contracting myofibrils, which have not been seen by any other study.

Relationship to Other Structural Data. EM studies on scallop myosin, using negative staining, have indicated that the myosin heads have an ordered helical arrangement in the relaxed state (*58*). Upon addition of activating concentrations of calcium to these filaments, the arrangement became disordered. Superficially, this would seem to be in conflict with our anisotropy data showing a large rotational movement in the head in relaxed myofibrils. This apparent discrepancy probably arises because electron microscopy detects static structural states in stained samples, while TPA detects dynamics in unfixed samples. Recent cryo-electron microscopy studies, which do not involve any fixing, suggest that the myosin head adopts a wide range of orientations during relaxation, both in the S1 form and in fibers (*8*, *9*), in agreement with our results.

EPR of spin-labeled gizzard RLC has shown that contraction of scallop adductor muscle involves a shift of the LC domain by at least 36° (*32*). This study showed that scallop muscle fibers have two LC domain orientations, corresponding to two structural states M1 and M2, which differ in spin-label orientation by 36°. Transitions between the physiological states of rigor, relaxation, and contraction were accompanied by changes in the population distribution of M1 and M2. The M2 population increased as strong binding to actin was increased, from 50% in relaxation to 67% in contraction and 92% in rigor, so that increased strong binding corresponded to increased orientational order. This is consistent with the present study, in which increased strong binding correlates with decreasing amplitudes and rates of motion. Both of these RLC studies, as well as previous studies of catalytic domain orientation and dynamics (*59*), indicate that only a small fraction of the heads changes its orientation and dynamics from relaxation to contraction. The fraction of heads changing their orientation upon contraction was 17% in the EPR study (*32*), while our estimate in the present study is 24% (discussed above), and previous probe studies of the catalytic domain have yielded estimates in the range 10−30% (*59*). These results indicate that *a snapshot of a muscle fiber in isometric contraction reveals only a small fraction of the heads in strong-binding, force-generating states.*

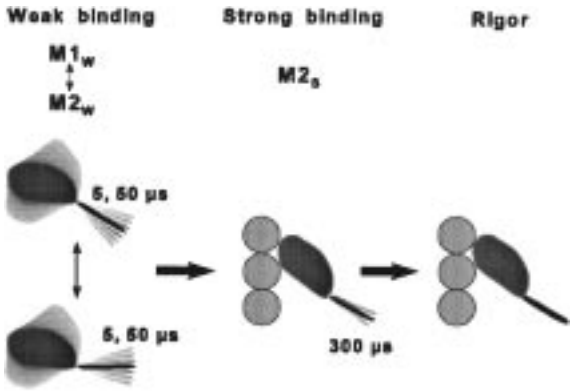

FIGURE 4: Molecular model of muscle contraction suggested by our results. This is a refinement of the model proposed by Baker et al. (*32*). Numbers at the LC domain represent the correlation times measured in our study. In relaxation (weak-binding state) both the catalytic and LC domains are dynamically disordered. However, unlike the catalytic domain, the LC domain is equally distributed between two distinct structural states (M_{1w} and M_{2w}). In contraction, strong binding to actin results in both domains becoming ordered, with the LC domain having greater mobility than the catalytic domain and being predominantly in the $M2_s$ structural state. In rigor, the catalytic domain has no rotational motion and the LC domain exhibits very little mobility.

Model of Contraction. We have used the results of the present study to refine a model of muscle contraction developed by Baker et al. (*32*, Figure 4). In this model, in the weak-binding states of relaxation, myosin exists as two structural states, M1 and M2, determined by the orientations of the LC domain, while the catalytic domain undergoes large amplitude motions as detected by both TPA and EPR studies (*59*). Our TPA data suggests that both these LC domain structures have substantial microsecond mobility (Figure 4, left). Progression into contraction is accompanied by the transition of a small fraction of the myosin heads from the weak-binding M1/M2 structural states to a strong binding M2 structural state, in which the LC domain has only one of the two orientations and the catalytic domain is immobile (Figure 4, middle). This state, which is only populated by about one-fourth of the heads in the steady state of contraction, has decreased microsecond mobility (correlation time about 300 μs) of the LC domain. Transition to rigor eliminates this slow motion in the LC domain, resulting in a strongly bound myosin head with very little motion in either domain. On the basis of this model, we propose that muscle contraction involves a disorder-to-order transition of both the catalytic and LC domains as well as a transition between distinct structural states of the LC domain.

Conclusions. In the present study, we have performed time-resolved phosphorescence anisotropy on scallop myofibrils, containing ErIA-labeled gizzard RLC, to delineate the rotational motions of the LC domain in the microsecond time scale. In rigor, only highly restricted microsecond motion occurs. In relaxation, large amplitude motions are seen, due to weak binding or complete detachment of the myosin head from actin. In contraction, in addition to a slight rise in anisotropy when compared to relaxation, a slow decay component is seen, indicating a rotational motion that is not present in either relaxation or rigor. This motion is associated with a transition of the myosin heads from the weak-binding

to the strong-binding states, with only a small fraction of the heads strongly bound to actin at one time. These results support a model of of muscle contraction that involves dynamic disorder-to-order transitions of both the domains of myosin head as well as a shift in the distribution between two LC domain orientations.

ACKNOWLEDGMENT

We thank Dr. Andrew Szent-Györgyi for providing protocols for scallop muscle preparation, Dr. Osha Roopnarine for helping to develop the technology for spectroscopic studies of scallop muscle in this laboratory, Dr. Osha Roopnarine and Leslie LaConte for critical reading of the manuscript, and Roberta Bennett and Nicoleta Cornea for technical assistance.

REFERENCES

1. Huxley, A. F. (1957) *Prog. Biophys. 7*, 255.
2. Reedy, M. K., Holmes, K. C., Tregear, R. T. (1965) *Nature 207*, 1276−1281.
3. Huxley, H. E. (1969) *Science 164*, 1356−1366.
4. Huxley, A. F., and Simmons, R (1971) *Nature 233*, 533−538.
5. Eisenberg, E., and Hill, T. L. (1985) *Science 227*, 999−1005.
6. Taylor, E. W. (1979) *Biochemistry 16*, 732−740.
7. Hibberd, M. G., and Trentham, D. R. (1986) *Annu. Rev. Biophys. Chem. 15*, 119−161.
8. Walker, M., White, H., Belknap, B., and Trinick, J. (1994) *Biophys. J. 66*, 1563−1572.
9. Hirose, K., Lenart, T. D., Murray, J. M., Franzini-Armstrong, C., and Goldman, Y. E. (1993) *Biophys. J. 65*, 397−408.
10. Pollard, T. D., Bhandari, D., Maupin, P., Wachsstock, D., Weeds, A. G., and Zot, H. (1993) *Biophys. J. 64*, 454−471.
11. Huxley, H. E. (1984) in *Contractile Mechanisms in Muscle* (Pollack, G. H., and Sugi, H., Eds.) pp 161−175, Plenum.
12. Wakabayashi, K., Tokunaga, M., Kohno, I., Sugimoto, Y., Hamanaka, T., Takezawa, Y., Wakabayashi, T., and Amemiya, Y. (1992) *Science 258*, 443−447.
13. Thomas, D. D. (1987) *Annu. Rev. Physiol. 49*, 691−709.
14. Berger, C. L., Svensson, E. C., and Thomas, D. D. (1989) *Proc. Natl. Acad. Sci. U.S.A. 86*, 8753−8757.
15. Berger, C. L., and Thomas, D. D. (1993) *Biochemistry 32*, 3812−3821.
16. Berger, C. L., and Thomas, D. D. (1994) *Biophys. J. 67*, 250−261.
17. Cooke, R., Crowder, M. S., and Thomas, D. D. (1982) *Nature 300*, 776−778.
18. Cooke, R. (1986) *CRC Critical Reviews in Biochemistry*, Vol. 21, pp 53−118, CRC Press, Boca Raton.
19. Fajer, P. G., Fajer, E. A., and Thomas, D. D. (1990) *Proc. Natl. Acad. Sci. U.S.A. 87*, 5538−5542.
20. Roopnarine, O., and Thomas, D. D. (1995) *Biophys. J. 68*, 1461−1471.
21. Svensson, E. C., and Thomas, D. D. (1986) *Biophys. J. 50*, 999−1006.
22. Root, D. D., and Reisler, E. (1992) *Biophys. J. 63*, 730−740.
23. Huxley, H. E., and Kress (1985) *J. Mus. Res. Cell Motil. 6*, 153−161.
24. Rayment, I., Rypniewski, W. R., Schmidt-Bäse, K., Smith, R., Tomchick, D. R., Benning, M. M., Winkelmann, D. A., Wesenberg, G., and Holden, H. M. (1993) *Science 261*, 50−58
25. Dominguez, R., Freyzon, Y., Trybus, K. M., and Cohen, C. (1998) *Cell 94*, 559−571.
26. Fisher, A. J., Smith, C. A., Thoden, J., Smith, R., Sutoh, K., Holden, H. M., and Rayment, I. (1995) *Biophys. J. 68*, 19s-28s.
27. Smith, C. A., and Rayment, I. (1996) *Biochemistry 35*, 5404−5417.
28. Taylor, K. A., Reedy, M. C., Córdova, L., and Reedy, M. K. (1984) *Nature 310*, 285−291.
29. Reedy, M. C., Reedy, M. K., and Goody, R. S. (1987) *J. Mus. Res. Cell Motil. 8*, 473−503.
30. Whittaker, M., Wilson-Kubalek, E. M., Smith, J. E., Faust, L., Milligan, R. A., and Sweeney, H. L. (1995) *Nature 378*, 748−751.
31. Rayment, I., Holden, H., Whittaker, M., Yohn, C., Lorenz, M., Holmes, K. C., and Milligan, R. (1993) *Science 261*, 58−65.
32. Baker, J. E., Brust-Mascher, I., Ramachandran, S., LaConte, L. E. W., and Thomas, D. D. (1998) *Proc. Natl. Acad. Sci. U.S.A. 95*, 2944−2949.
33. Chantler, P. D., and Szent-Györgyi, A. G. (1980) *J. Mol. Biol. 138*, 473−492.
34. Sellers, J., and Szent-Györgyi, A. G. (1980) *J. Mol. Biol. 144*, 223−143.
35. Roopnarine, O., Szent-Györgyi, A. G., and Thomas, D. D. (1998) *Biochemistry 37*, 14428−14436.
36. Ludescher, R. L., and Thomas, D. D. (1988) *Biochemistry 27*, 3343−3351.
37. Stein, R. A., Ludescher, R. D., Dahlberg, P. S., Fajer, P. G., Bennett, R. L. H., and Thomas, D. D. (1990) *Biochemistry 29*, 10023−10031.
38. Persechini, A., and Hartshorne, D. J. (1983) *Biochemistry 22*, 470−477.
39. Wagner, P. D. (1982) *Methods Enzymol. 85*, 72−81.
40. Bradford, M. M. (1976) *Anal. Biochem. 72*, 248−254.
41. Lanzetta, P. A., Alvarez, L. J., Reinach, P. S., Candia, O. A. (1979) *Anal. Biochem. 100*, 95−97.
42. Bevington, P. R. (1969) *Data Reduction and Error Analysis for the Physical Sciences*, McGraw-Hill, New York.
43. Kinosita, K., Kawato, S., and Ikegami, A. (1977) *Biophys. J. 20*, 289−305.
44. Ludescher, R. D., Eads, T. W., and Thomas, D. D. (1987) in *Optical Probes of Muscle Cross- bridges* (Baskin, R., and Yeh, Y., Eds.) pp 33−65, CRC Press, Boca Raton.
45. Kendrick-Jones, J., Lehman, W., and Szent-Györgyi, A. G. (1970). *J. Mol. Biol. 54*, 313−326.
46. Fromherz, S., and Szentgyörgyi, A. G. (1995) *Proc. Natl. Acad. Sci. U.S.A. 92*, 7652−7656.
47. Houdusse, A., and Cohen, C. (1996) *Structure 4*, 21−32.
48. Xie, X., Harrison, D. H., Schlichting, I., Sweet, R. M., Kalabokis, V. N., Szent-Györgyi, A. G., and Cohen, C. (1994) *Nature 368*, 306−312.
49. Barnett, V. E., and Thomas, D. D. (1989) *Biophys. J. 56*, 517−523.
50. Allen, T., Ling, N., Irving, M., and Goldman, Y. E. (1996) *Biophys. J. 70*, 1847−1862.
51. Szent-Györgyi, A. G. (1996) *Biophys. Chem. 59*, 357−363.
52. Sabido-David, C.; Hopkins, S. C., Saraswat, L. D., Lowey, S., Goldman, Y. E., and Irving, M. (1998) *J. Mol. Biol. 279*, 387−402.
53. Hambly, B., Franks, K., and Cooke, R. (1991) *Biophys. J. 59*, 127−138.
54. Hambly, B., Franks, K., and Cooke, R. (1992) *Biophys. J. 63*, 1306−1313.
55. Zhao, L., Gollub, J., and Cooke, R. (1996) *Biochemistry 35*, 10158−10165.
56. Ling, N., Shrimpton, C., Sleep, J., Kendrick-Jones, J., and Irving, M. (1996) *Biophys. J. 70*, 1836−1846.
57. Irving, M., Allen, T. St. C., Sabido-David, C., Craik, J. S., Brandmeier, B., Kendrick-Jones, J., Corrie, J. E. T., and Goldman, Y. E. (1995) *Nature 375*, 688−691.
58. Vibert, P., and Craig, R. (1985) *J. Cell Biol. 101*, 830−837.
59. Thomas, D. D., Ramachandran, S., Roopnarine, O., Hayden, D. W., and Ostap, E. M. (1995) *Biophys. J. 68*, 135s-141s.

BI9902945